American Journal of
Physical Science
(AJPS)

Theoretical and Experimental Study of the Adsorption of Natural Red 4 Dye from Synthetic Aqueous Media Using a Low-cost Silica-smectite Composite

Jean Marie Kepdieu, Chantale Njiomou Djangang, Jacques Romain Njimou, Gustave Tchanang, Cyprien Joel Ekani, Sanda Andrada Maicaneanu and Chedly Tizaoui

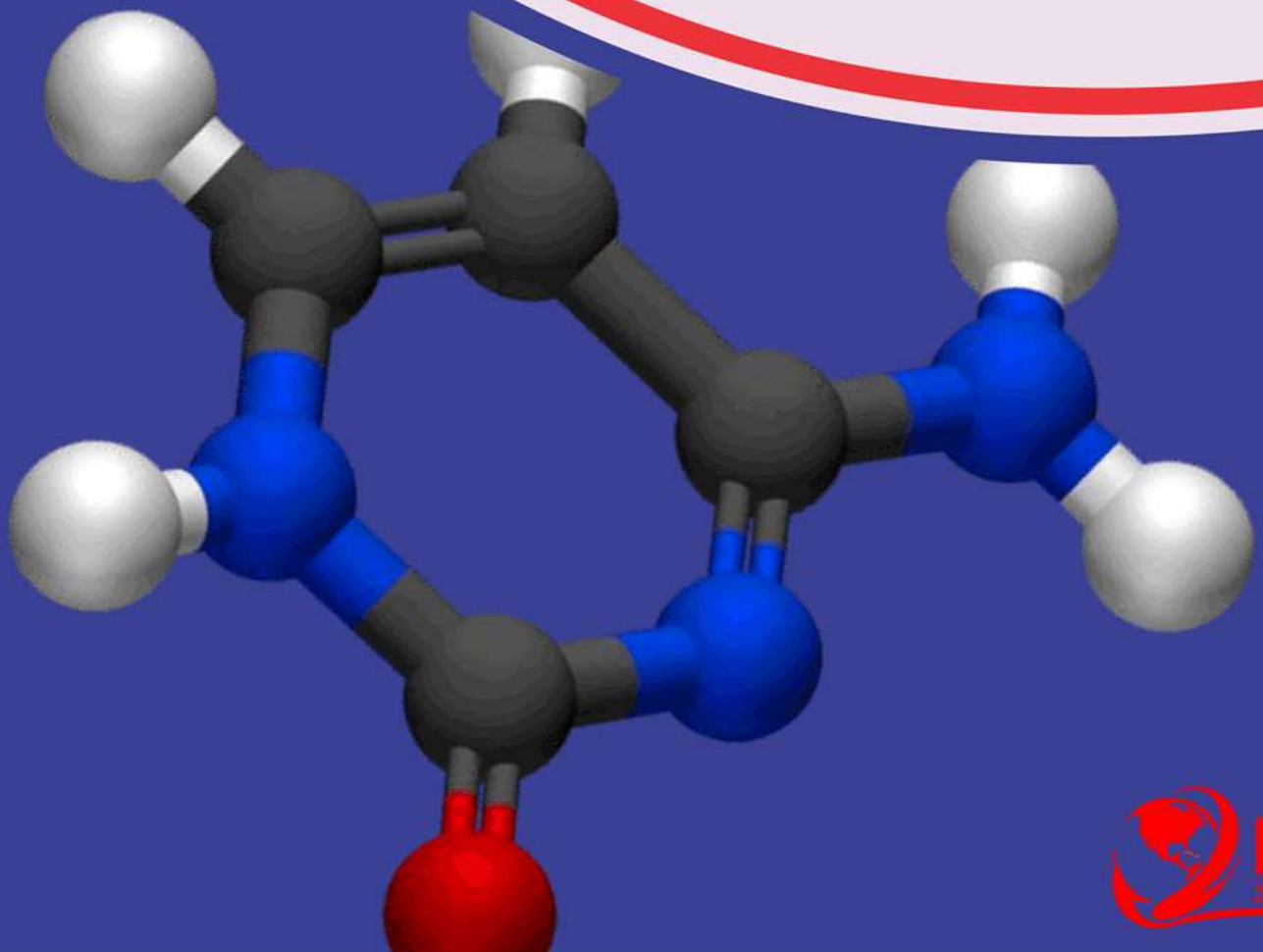

IPRJB

American Journal of Physical Sciences
ISSN: 2958-969X (Online)
Vol. 1, Issue 2, No. 1, pp 1 - 21, 2023

www.iprjb.org

Theoretical and Experimental Study of the Adsorption of Natural Red 4 Dye from Synthetic Aqueous Media Using a Low-cost Silica-smectite Composite

Jean Marie Kepdieu*[a], Chantale Njiomou Djangang[a] Jacques Romain Njimou[b,c], Gustave Tchanang[a], Cyprien Joel Ekani[a] Sanda Andrada Maicaneanu[c] and Chedly Tizaoui[d]

[a]Department of Inorganic Chemistry, University of Yaoundé I, Cameroon.
[b]School of Chemical Engineering and Mineral Industries, University of Ngaoundéré, Ngaoundéré, Cameroon.
[c]Madia Department of Chemistry, Biochemistry, Physics and Engineering, Indiana, University of Pennsylvania, Indiana, USA.
[d]Department of Chemical Engineering, Swansea University, Bay Campus, Fabian Way, Swansea SA1 8EN, UK.

Article History

Received 10th September 2023
Received in Revised Form 22nd September 2023
Accepted 6th October 2023

How to cite in APA format:
Kepdieu, J., Djangang, . C., Njimou, J., Tchanang, G., Ekani, C. ., Maicaneanu, S., & Tizaoui, C. (2023). Theoretical and Experimental Study of the Adsorption of Natural Red 4 Dye from Synthetic Aqueous Media Using a Low-cost Silica-smectite Composite. *American Journal of Physical Sciences*, *1*(2), 1–22. https://doi.org/10.47604/ajps.2137

Abstract

Purpose: A study of the removal of dye Natural red 4 (NR4) by a low-cost silica-smectite clay labeled SSC was carried out.

Methodology: Batch tests were carried on with some processing parameters namely initial dye concentration (10 - 50 mg/L), temperature (25 – 65 °C), adsorbent dose (1 – 5 g/L), initial pH (4 – 8) and contact time (0 - 120 min).

Findings: The Energy of adsorption was less than 20 kJ/mol showing a physisorption process. Also, thermodynamics parameters such as enthalpy of activation ΔH* (19.0 kJ/mol), entropy of activation ΔS* (- 024 kJ/mol/K) and Gibbs free energy of activation ΔG* (90.57 - 100.17 kJ/mol) revealed that the adsorption of NR4 molecules onto SSC was endothermic and with no significant changes in the internal structure of the adsorbent. The pseudo-first order and pseudo-second order had a good correlation with experimental data with R^2 = 0.99 and R^2 = 0.98 respectively. Langmuir isotherm model matched well the equilibrium data with a maximum adsorption capacity Q_m of 25.55 mg/g. and a correlation value of 0.98.

Unique Contribution to Theory, Policy and Practice: The newly synthesized and characterized low-cost silica-smectite composite is effective in the adsorptive removal of natural red 4 dye from water wastes.

Keywords: *Adsorption, Dye, Natural Red 4, Thermodynamic and Kinetics*

American Journal of Physical Sciences
ISSN: 2958-969X (Online)
Vol. 1, Issue 2, No. 1, pp 1 - 22, 2023
www.iprjb.org

INTRODUCTION

Anthropogenic activities such as paint, manufacturing, textile, cosmetics, plastics, food, paper and leather are responsible for the discharge of coloured dyes in receiving waters [1]. Some dyes in water hinder the penetration of light resulting in significant changes in the turbidity, colour and transparency of water and disturbance of ecosystem. Those which are not visible can be transformed into toxic or carcinogenic compounds after long time exposure [1–5]. They also affect negatively the human life by affecting vital activities such as drinking, washing and bathing and are responsible for dysfunction in the brain and central nervous system, liver, kidney, reproductive system, and cancer [6–8]. The chemical structures of those dyes generally contains aromatic groups and metals which enable them to be less or not biodegradable [9–11]. Natural Red 4 (NR4) is a red glucosidal hydroxyanthrapurin that occurs naturally in some scale insects, such as the cochineal, Armenian cochineal, and Polish cochineal. [12,13]. It is an anionic, anthraquinone dye that is relatively water soluble. It is widely used in textile, cosmetics, printing, food industry, medical and pharmaceutical applications [14]. It has been found to be toxic and neurotoxic and cause skin and eye diseases and cancer in case of considerable intakes.

The primary concern worldwide has been the maintenance of adequate and good water quality [7]. It is then of great interest to find ways for effective removal of NR4 from industrial wastewaters before discharging them into environment. For instance, several techniques among which coagulation, chemical oxidation, membrane separation, and electrochemical, aerobic, and anaerobic microbial degradation are often used but not widely due to their high cost and high selectivity [15,16]. Adsorption is then mostly applied to treat dye containing wastewater because of its low cost, flexible and simple design, resistance to toxic substances, and high efficiency [5,17–19]. Nowadays, the use of renewable, cheap, and abundant agricultural wastes as adsorbents has been reported by many authors and their efficiency also proved [19–21]. Two bioresourced materials, rice husk and smectite clay have been widely studied and are classified as mesopourous materials with good surface properties. They have been used in a previous work to synthesize a low-cost silica-smectite composite [22]. The current work aims to apply the so-called composite in the removal of NR4 from synthetic aqueous media using batch methods. Such composite has been never used for the adsorption of NR4. It is thus important to evaluate its efficiency. Some processing parameters such as contact time, pH effect, adsorbent dosage, dye initial concentration, and temperature will be investigated in order to enlighten the adsorption equilibrium, kinetic and thermodynamic of process.

MATERIALS AND METHODS

Adsorbent

The adsorbent used in this study was synthesized using a 20 µm mesh enriched smectite clay fraction and silica from rice husk ash as starting materials. It led to a product which structure was described in a previous study [22] as a delaminated/exfoliated mesoporous material with a specific surface area of 257 m^2/g. In this study, that composite is labelled SSC (Silica-smectite composite). In order to determine the pH zero point charge (pH_{zpc}), an electro-chemical method reported by some workers [23,24] has been used: 50 mL of 0.1 N NaCl solutions was placed in 100 mL erlenmeyer flasks. The pH was firstly adjusted to successive initial values between 2 and 12 by using either 0.1 N NaOH or HCl solutions and secondly, 0.10 g of SSC was added to the solutions. After a contact time of 48 hours under stirring, the final pH_f was plotted against the initial pH_i and the intersection point of the curve with the bissector line corresponds to the

pH_{zpc} value of SSC. All pH measurements have been made with a digital pH meter, type CT-6023.

Adsorbate

Naturel Red 4 also called (1S)-1, 5-Anhydro-1-(7-carboxy-1, 3, 4, 6-tetrahydroxy-8-methyl-9,10-dioxo-9,10-dihydroanthracen-2-yl)-D-glucitol, purchased from Sigma (90% pure), was analytical reagent grade and was used as received. 1000 mL of 200 mg/L stock solution was prepared. Other solutions of desire concentrations were prepared by simple dilution of the stock one. The chemical structure of NR4 is shown in **Fig. 1b**. It contains a carboxylic acid and phenolic groups. In aqueous solution, it ionizes to an anionic, colored component and H^+ cations [2,25]

Adsorption Experiments

The influence of some processing parameters such as contact-time, temperature, initial concentration and adsorbent dose on the adsorption of NR4 onto SSC has been investigated through batch experiments.

For the influence of contact time and temperature, 20 mL of NR4 solution with initial concentration of 50 mg/L and 0.04 g of SSC was introduce in the flask at t = 0 The mixture was stirred in a thermostated water bath system at a constant speed of 250 rpm at different temperatures (25 – 65 °C) and contact-time (0 - 120 min).

For the influence of adsorbent dose, the latter was varied from 1 to 5 g/L (precisely, 0.02 – 0.1 g for the 20 mL dye solution).For equilibrium studies, the initial concentration was varied from 10 – 100 mg/L at pH = 6 and temperature of 65°C. The effect of initial pH was studied in the range of 4.0 – 8.0 knowing that the pH point zero charge (pH_{zpc}) is firstly determined.

At each turn, the adsorbent was separated from solution and the concentration of NR4 dye in the solution before and after adsorption were determined by UV Vis spectrophotometry (Spectro Direct AQUALYTIC), at a wavelength of 497 nm previously determined by drawing the absorbance spectrum of NR4 shown on **Figure 1a.** A calibration curve (**Figure 1c**) is also drawn by making serial dilutions and then plotting the absorbance against concentration at the maximum wavelength prior to further experimentations.

For reusability evaluation, 3 adsorption/desorption cycles were carried out, the desorption experiments were carried out in H_2O, H_2SO4 and C_2H_5OH solutions of 0.1 mol/L concentration to recover the NR4 dye adsorbed on the SSC surface. At the end of the experiment, the solution was centrifuged and concentration of NR4 dye recovered after desorption process was determined by spectrophotometric measurements and the Recovery percentage (Rc (%)) was calculated. Desorption experiments were performed by dispersing 10 mg of NR4-loaded SSC in 10 mL under magnetic stirring at room temperature for 30 min. Then, the solids were centrifuged at 2500 rpm for 5 min. Finally, the amount of dye remaining in the supernatant was determined by UV–Vis spectroscopy and the amount of dye (Q_{des}) in the supernatant after desorption was determined [26].

American Journal of Physical Sciences
ISSN: 2958-969X (Online)
Vol. 1, Issue 2, No. 1, pp 1 - 22, 2023
www.iprjb.org

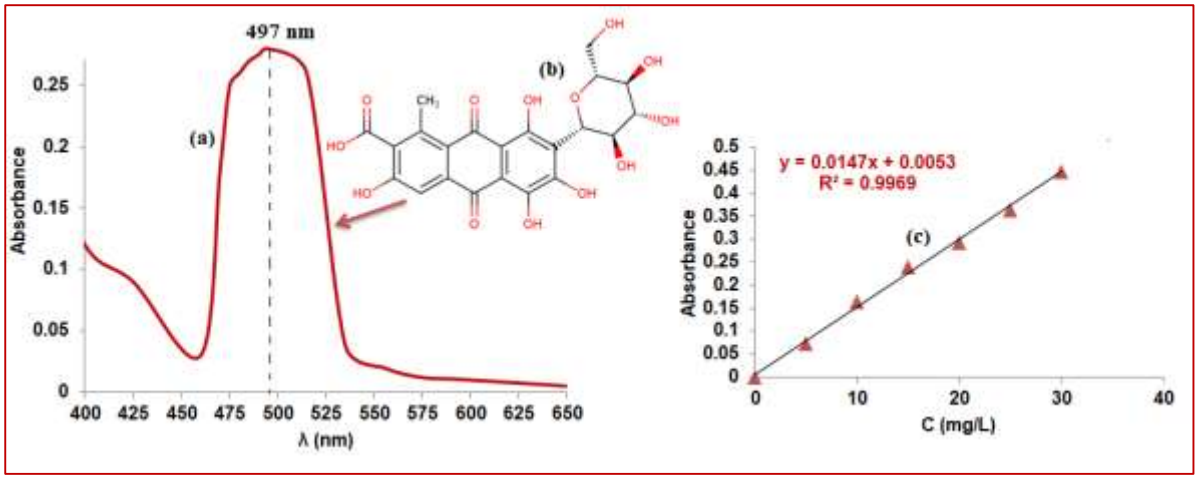

Figure 1: Absorption Spectrum (a), Topological Molecule of NR4 (b) and Calibration Curve (c)

Theoretical Studies

Assay on Adsorption and Desorption Parameters

Eqs. 1, **2, 3** and **4** were used for the calculations of the adsorption capacity at time t (Q_t), at equilibrium (Q_e), the removal yield (R (%)) and the recovery yield ((Rc (%)) respectively. Duplicate experiments were carried out for all the operating variables studied and only the average values were taken into consideration.

$$Q_t = \frac{(C_0 - C_t).V}{m} \quad (1)$$

$$Q_e = \frac{(C_0 - C_e).V}{m} \quad (2)$$

$$R\ (\%) = \frac{(C_0 - C_t).V}{m} \text{ x } 100 \quad (3)$$

$$Rc\ (\%) = \frac{Q_{des}}{Q_{ads}} \text{ x } 100 \quad (4)$$

Where C_0, C_t and C_e are the initial, time t (min) and equilibrium dye concentrations (mg/L), respectively. V is the volume of solution (L), m the mass of adsorbent used (g), Q_{des} the amount of NRA recovered (mg/g) and Q_{ads}, the amount of NR4 adsorbed (mg/g).

Kinetics and Thermodynamics

In order to elucidate the mechanism of adsorption of NR4 onto SSC, the experimental data have been compared to the theoretical models of pseudo-first order, pseudo-second order, and intraparticle diffusion which are commonly used in the adsorption of dyes [27–31]

Pseudo-First Order Kinetic Model

The non-linear and linear forms of the pseudo-first order kinetic modeling are given by **Eqs. 5** and **6**.

$$Q_{t=Q_e(1-Exp^{(-k_1 t)}} \quad (5)$$

$$\ln(Q_e - Q_t) = \ln Q_e - k_1 t \quad (6)$$

k_1 (min^{-1}) is the kinetic constant of the first order kinetic, t (min) is the time; Q_e and Q_t (mg/g) represent the amounts of β-carotene adsorbed at equilibrium and at time t respectively.

American Journal of Physical Sciences
ISSN: 2958-969X (Online)
Vol. 1, Issue 2, No. 1, pp 1 - 22, 2023
www.iprjb.org

Pseudo-Second-Order Kinetic Model

Eq. 7 and **8** represent the non-linear and linear forms of the pseudo-second order kinetic modeling

$$Q_t = \frac{K_{2Q_e^2 t}}{1+K_2 Q_e t} \quad (7)$$

$$\frac{t}{Q_t} = \frac{1}{K_2 Q_e^2} + \frac{t}{Q_e} \quad (8)$$

Where K_2 ($mg^{-1}g.min$) is the pseudo-second order kinetic constant.

Intraparticle Diffusion Kinetic Model

The Weber–Morris intraparticle diffusion model is expressed in **Eq. 9**.

$$Q_t = K_{id} t^{1/2} + \gamma \quad (9)$$

Where k_{id} ($mg/gmin^{0.5}$) is the intra-particle diffusion rate constant and $\boldsymbol{\gamma}$ (mg/g) is associated to the boundary thickness. The line must go through the origin if intra-particle diffusion is the only rate-limiting step [15,32].

Energies of Activation and Thermodynamics Parameters

The type of adsorption process can be also determined by the value of the activation energy involved during the process.For a physisorption process, the activation energies range between 5 and 40 $kJ.mol^{-1}$ while for a chemisorption process they range between 40-800 $kJ.mol^{-1}$ [33] .

The linear forms of Arrhenius and Eyring's plots are given in **Eqs. 10** and **11** [25,34,35] were used for the determination of the activation energy Ea (kJ/mol), the enthalpy of activation ΔH* (kJ/mol) and the entropy of activation ΔS* (kJ/mol/K).

$$\ln K_2 = \ln A - \frac{E_A}{RT} \quad (10)$$

$$\ln \frac{K_2}{T} = \left(\ln \frac{K_B}{h} + \frac{\Delta S^*}{R}\right) - \frac{\Delta H^*}{RT} \quad (11)$$

The Gibbs free energy of activation ΔG* (kJ/mol) was calculated from **Eq.12**.

$$\Delta G^* = \Delta H^* - T\Delta S^* \quad (12)$$

where K_2 is the rate constant of the pseudo-second order, A is the pre-exponential factor, R (J.mol/K) is the gas constant, T ($°K^{-1}$) is the operated temperature, K_B (J/K) is the Boltzmann constant and h (J.s) the Plank constant.

Equilibrium Study

The relation between the amount of a substance removed from the liquid phase by a unit mass of adsorbent and its concentration at a constant temperature is known as adsorption isotherms. Two models were used to determine the best interpretation of the process of the adsorption of NR4 on SSC. The data obtained provided a better understanding of the adsorption mechanism and its characteristics.

The non-linear and linear equations of the Langmuir model are given by **Eqs. 13** and **13**.

American Journal of Physical Sciences
ISSN: 2958-969X (Online)
Vol. 1, Issue 2, No. 1, pp 1 - 22, 2023
www.iprjb.org

$$Q_e = \frac{Q_m K_L C_e}{1+K_L C_e} \quad (13)$$

$$\frac{C_e}{Q_e} = \frac{1}{Q_m K_L} + \frac{C_e}{Q_m} \quad (14)$$

Where Q_e is the amount of dyes adsorbed per gram of adsorbent, C_e the residual amount of dye at equilibrium, Q_m the maximum amount of adsorbed substance, and K_L a constant reflecting the affinity of the adsorbed for the adsorbent.

The non-linear and linear equations of Freundlich model are given by **Eqs. 15** and **16**.

$$Q_e = K_F C_e^{\frac{1}{n}} \quad (15)$$

$$\log(Q_e) = \frac{1}{n}\log C_e + \log K_F \quad (16)$$

Where K_F is the constant reflecting the measurement of the capacity of adsorption, and n is the constant reflecting the affinity of the adsorbate for the adsorbent; Q_e is the amount of dye adsorbed per gram of adsorbent and C_e is the concentration of dye at equilibrium.

Validation of the Model

Using a statistical method involving Correlogram plots and scatterplots obtained from Minitab21Sofwaure©, the correlation values R^2 were estimated between the experimental data and the kinetic and isotherm models. The best fitting to a model with good accuracy is generally obtained with R^2 values greater than 95% [36].

RESULTS AND DISCUSSION

Contact Time and Temperature

The effect of contact time (0 – 120 min) and temperature (25 – 65°C) on the adsorption of NR4 onto SSC is shown on Figure 2.

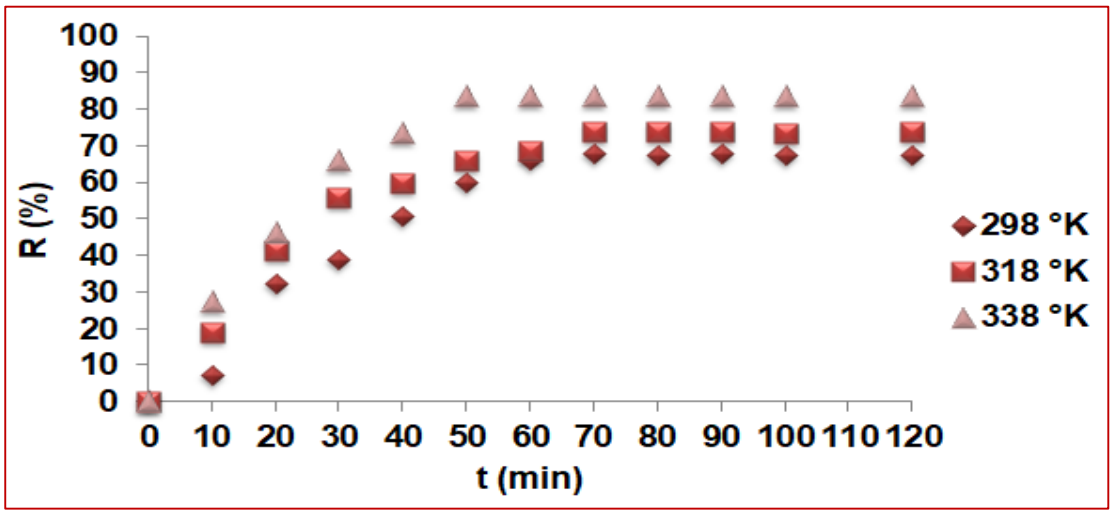

Figure 2: Plots of the Effect of Contact-Time and Temperature on the Adsorption of NR4 on SSC

American Journal of Physical Sciences
ISSN: 2958-969X (Online)
Vol. 1, Issue 2, No. 1, pp 1 - 22, 2023
www.iprjb.org

For each temperature, the amount of dye adsorbed increases with increasing contact time. There is a rapid adsorption of NR4 in the first 30 min followed by the gradual increase of adsorption rate and ultimately reaches a steady step. The initial rapid phase may be due to high concentration of vacant sites of the adsorbent at the initial stage and the steady step is due to the saturation [37,38]. The Equilibrium time is found to decrease with increasing temperature having the values of 80 min, 70 min and 60 min at 25°C, 45°C and 65°C respectively. This trend is due to the rising of kinetic energy with temperature, favorable to distribution of SSC particles into the solution on one hand and the activation of sites on the other hand.

Adsorbent Dose

The effect of SSC dose was studied in range of 1–5 g/L for dye concentration of 50 mg/L and pH 5.

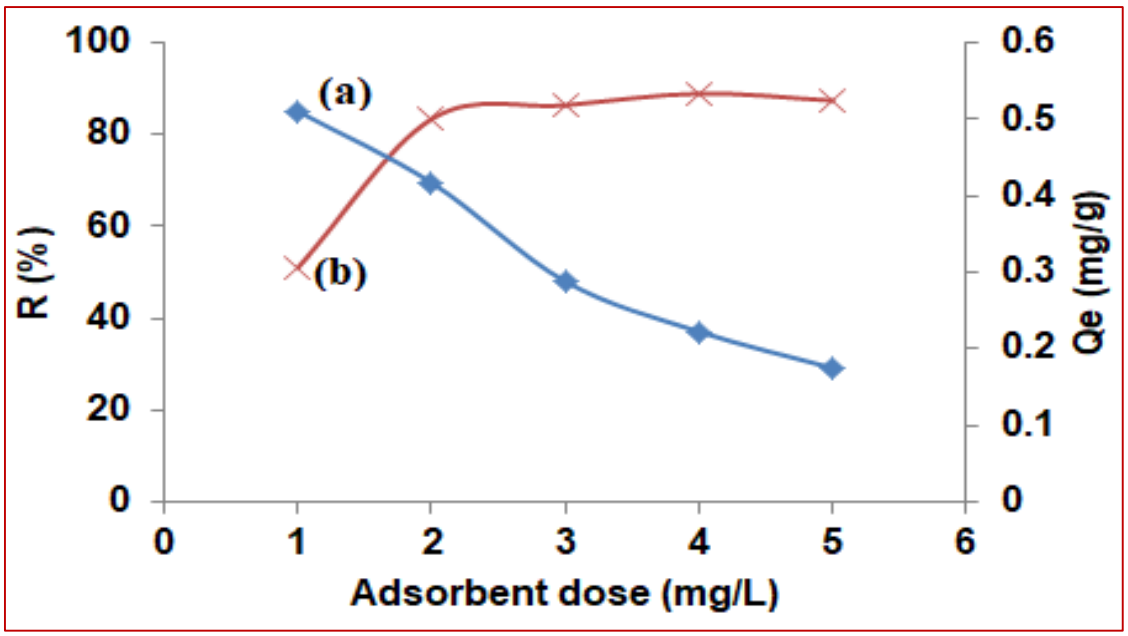

Figure 3: Plots of the Effect of Adsorbent Dose on the Adsorption Capacity (a) and Percentage of Dye Removal (b)

The results presented on **Fig. 3** shows that the percent removal of NR4 increases from 51.06 to 87.45 % while the adsorption capacity decreases from 0.5 to 0.17 mg/g when the adsorbent dose rises from 1 to 5 g/L. In fact, the larger the mass of the adsorbent used, greater the availability of more adsorption sites [27,38,39]. Inversely, the amount adsorbed per unit of adsorbent decreases and can be attributed to the unsaturation of active sites on the adsorbent surface [7].

Point Zero Charge and Effect of Initial pH

The point zero charge was found as the point of intersection between **Figure 4a** and **Figure 4b** corresponding to 6.64. The influence of the initial pH on the adsorption of NR4 by SSC is plotted (**Figure 4c**).

American Journal of Physical Sciences
ISSN: 2958-969X (Online)
Vol. 1, Issue 2, No. 1, pp 1 - 22, 2023
www.iprjb.org

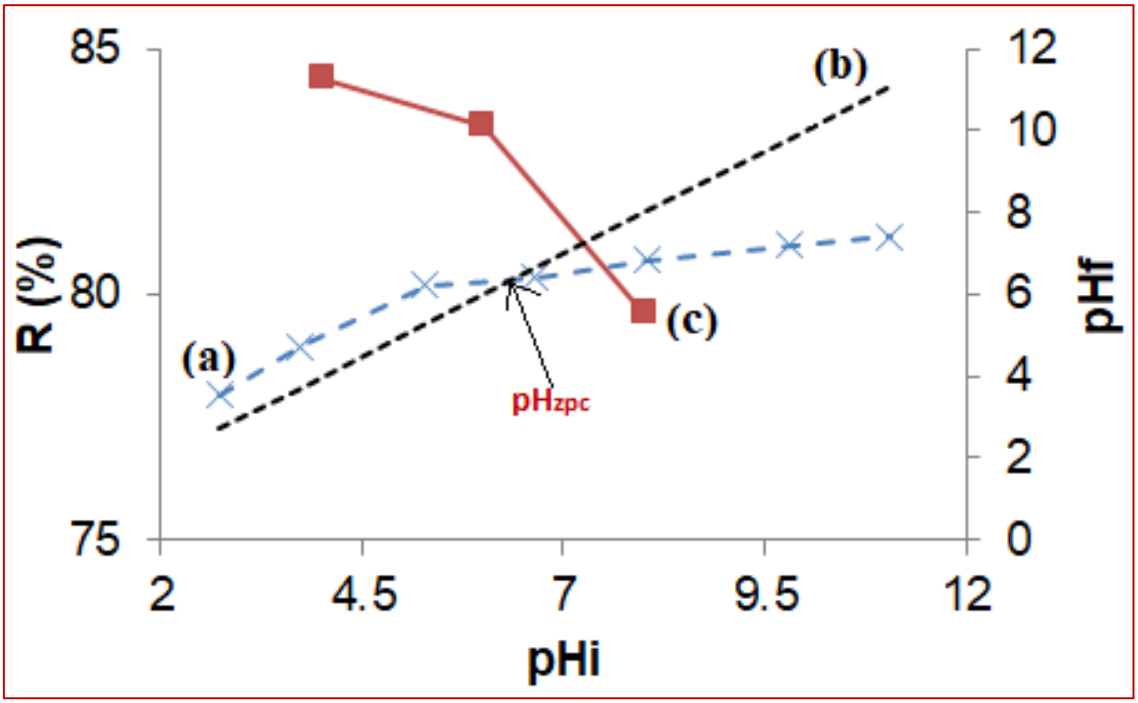

Figure 4: Plot of Final pH_f versus Initial pH_i (a), First Bisector Line (b) and Percentage Removal versus Initial pHi (c) for the Adsorption of NR4 onto SSC

Figure 4c shows a slight decrease of percentage removal from 84.39 to 79.63 % with the increase of initial pH from 4 to 8. The pH may affect the surface charge of SSC and also the ionization of the solution [39]. At low pH values (lower than pH_{zpc}), the surface silanols (-Si-OH) and aluminols (-Al-OH) groups of SSC may react with the oxoniums ions in solution following **Eq.6** and gain positive charges. This is then favorable to the adsorption of anionic NR4 due to attractive columbic forces. Inversely, at high pH values (greater than pH_{zpc}) the surface gains negative charge density (**Eq. 7**) and a reverse phenomenon is noticed. Similar trend has been observed by other workers for the adsorption of ionic dye on various materials [7,24,39–41].

$$SSC\text{-}M\text{-}OH + H_3O^+ \leftrightarrow (SSC\text{-}M\text{-}OH_2)^+ + H_2O \quad (M = Si, Al,\ pH < pHzpc) \quad (6)$$

$$SSC\text{-}M\text{-}OH + OH^- \leftrightarrow SSC\text{-}M\text{-}O^- + H_2O \quad (M = Si, Al, pH > pHzpc) \quad (7)$$

The anionic group is attracted by the positively charged $SSC\text{-}M\text{-}OH_2^+$ sites. The dye anion will suffer coulombic repulsion upon approaching the surface due to the presence of $SSC\text{-}M\text{-}O^-$.

Kinetics and Modeling Fitting

The kinetic of NR4 adsorption on SSC was studied at an initial concentration of 50 mg/L, 2 g/L as adsorbent dose and pH = 6. Three kinetic models, pseudo-first-order, pseudo-second-order and intra-particle diffusion were investigated. The non-linear regression of the models was carried out. The plots and the obtained kinetic parameters are presented in **Figure 5** and **Table 1** respectively. The correlation between the experimental data and the different models was statistically evaluated using correlogram plots and scatterplots shown in **Figure 6** and **7**.

American Journal of Physical Sciences
ISSN: 2958-969X (Online)
Vol. 1, Issue 2, No. 1, pp 1 - 22, 2023
www.iprjb.org

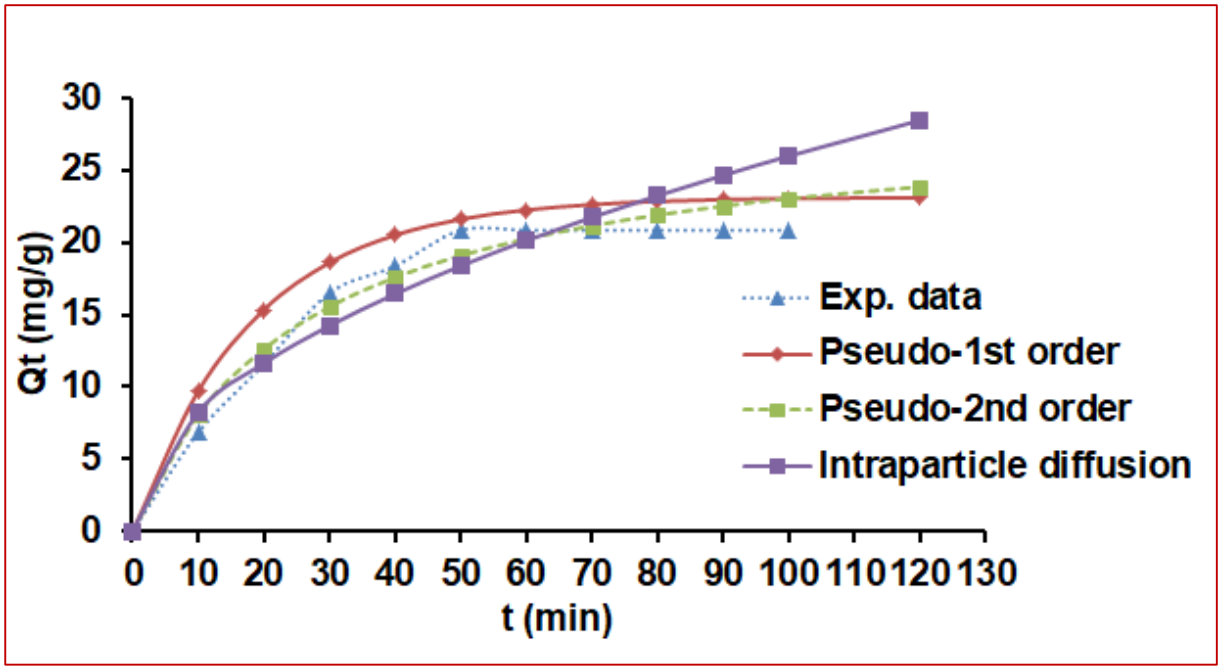

Figure 5: Non-linear Plots of Pseudo-First Order, Pseudo-Second Order and Intra-Particle Diffusion Models for the Adsorption of NR4 onto SSC

It appears on the correlogram of **Figure 6** that the pseudo-first order and the pseudo-second order fitted well the experimental data with correlation values of 0.99 and 0.98 respectively. The correlation with intraparticle diffusion model is less significant (0.93).

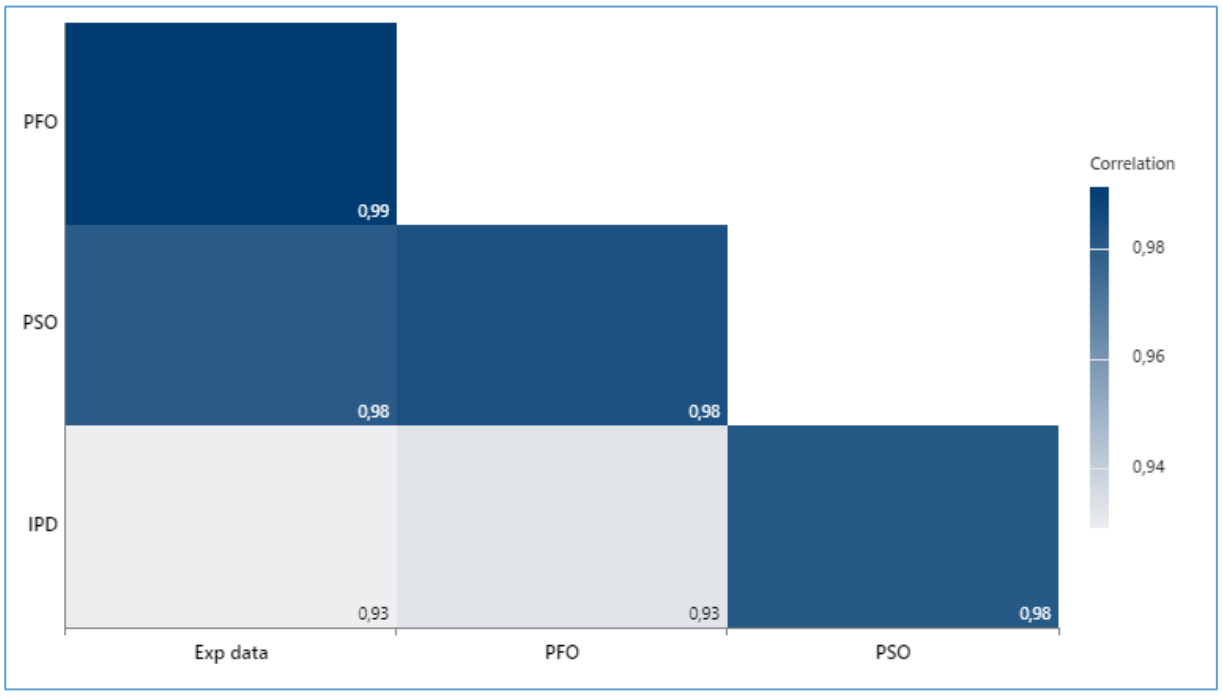

Figure 6: Correlogram Plots of Exp Data, Pseudo-First Order (PSO), Pseudo-Second Order (PSO) and Intraparticle Diffusion (IPD) Models

American Journal of Physical Sciences
ISSN: 2958-969X (Online)
Vol. 1, Issue 2, No. 1, pp 1 - 22, 2023
www.iprjb.org

The results are in accordance with the scatterplots presented in **Figure 7**. It can be observed that almost all the dots are near the straight line for the pseudo-first order and pseudo-second order models. Inversely, the dots are very scatter around the line for the intraparticle diffusion model. Nevertheless, it is noticed that in the parameter ranges, the fitting of the three kinetic models are competitive.

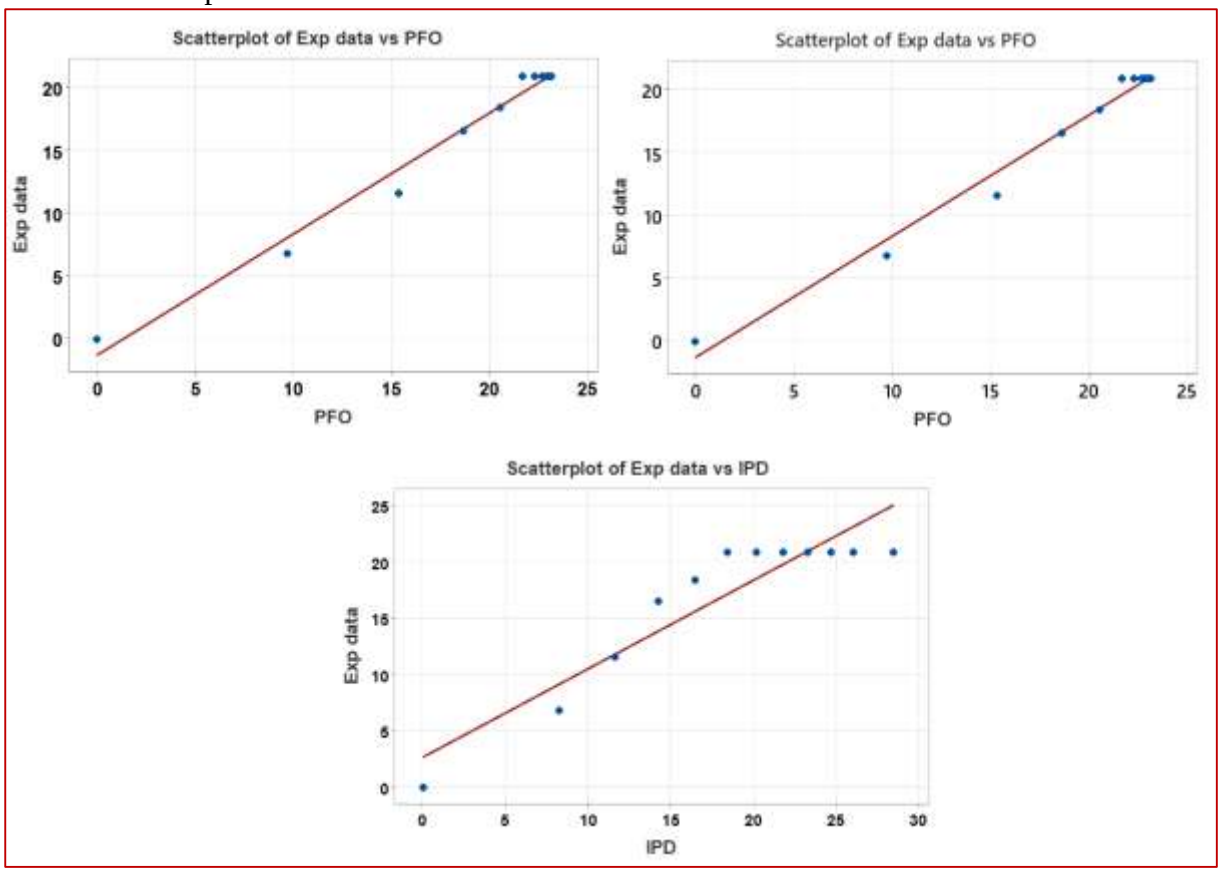

Figure 7: Statistical Scatterplots of Exp Data vs PFO, Exp Data vs PSO and Exp Data vs IPD

Table 1: Kinetic Parameters of the Adsorption of NR4 onto SSC

Pseudo-first order		Pseudo-second order		Intraparticucle diffusion	
$Q_{t=Q_e(1-Exp(-K_1t)}$		$Q_t = \frac{K_{2Q_e^2t}}{1+K_2Q_et}$		$Q_t = K_{id}t^{1/2} + \gamma$	
K_1 (min^{-1})	0.0543	K_2 (g/mg/min)	0.0013	K_{id} ($mg/g.min^{1/2}$)	2.597
Q_{exp} (mg/g)	20.86	Q_{exp} (mg/g)	20.86	Qexp (mg/g)	20.86
Q_e cal (mg/g)	22.160	Q_ecal (mg/g)	22.62	Q_e cal (mg/g)	23.25
R^2	0.99	R^2	0.98	R^2	0.93

K_1, K_2 and k_{id} are the kinetic constant of the 1st order, 2nd order and intra-particle diffusion kinetic constant respectively. γ (mg/g) is associated to the boundary layer thickness; t (min) is

the time; Q_e and Q_t represent the amounts of dyes adsorbed at equilibrium and at time t respectively.

The Pseudo-second order kinetic constant has been evaluated at three temperatures 298; 318 and 338°K. The results obtained allow the determination of Energy of activation Ea (kJ/mol), the enthalpy of activation ΔH* (kJ/mol), the entropy of activation ΔS* (kJ/mol/K) and the Gibbs free energy of activation ΔG* (kJ/mol).

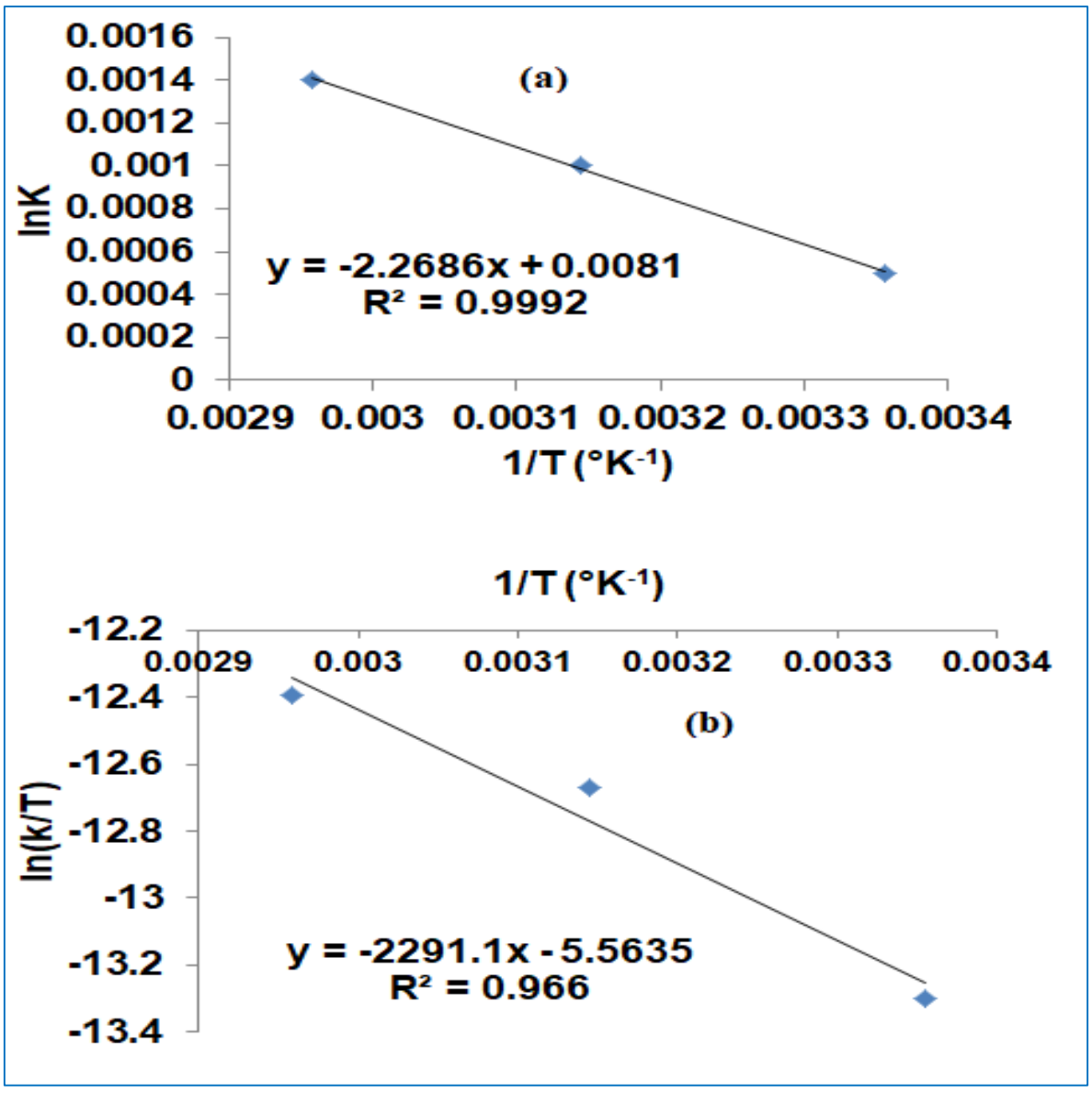

Figure 8: Plot of the Linear Forms of Arrhenius (a) and Eyring Equations (b)

Table 2: Activation Energy Parameters for Adsorptive Removal of NR4 on SSC

Ea (kJ/mol)	R^2	ΔH* (kJ/mol)	R^2	ΔS* (kJ/mol/K)	T (°K)	ΔG* (kJ/mol)
19.95	0.999	19.05	0.966	-0.24	298	90.57
					318	95.35
					338	100.17

The positive values of ΔH* and ΔG* seen from Table 2, indicate the presence of an energy barrier in the adsorption process [25]. Similar results for activation parameters have been reported for dye adsorption onto silica gel [42,43]. An approach found in the literature to interpret such results claiming the near to pH zero point charge which allow both anion and cation adsorption. The negative value of ΔS* indicates that, as a result of NR4 adsorption, no significant changes occur in the internal structure of the SSC [25].

Equilibrium and Modelling Fitting

The non-linear regression of the Langmuir and Freundlich isotherms and their corresponding constants are given in Figure 9 and Table 3 respectively. Between the two isotherm models studied and the equilibrium parameters determined, it appears that Langmuir isotherm model fitted well the experimental data of the adsorption of NR4 onto SSC with a coefficient of correlation R^2 of 0.98 as presented in the correlogram plot of Figure 10. A similar result is reported by many authors concerning the adsorption of dyes onto low-cost materials [1,7,38]. This also assumes that adsorption is limited to the formation of monolayer coverage of adsorbate on homogeneous adsorbent surface. This can be explained by the repulsion electric forces between some linked NR4 molecules and free ones. This phenomenon may limit the formation of multilayers. Futhermore, the values of the separation factor R_L are between 0.05 and 0.20. This essential characteristic of Langmuir isotherm defined by $R_L = 1/ (1 + K_L C_o)$ has been reported by many authors to indicate that the adsorption is favorable to Langmuir isotherm model when $0 < R_L < 1$ [36,44,45]. The scatterplots on Figure 11 also corroborates the prediction of Figure 10 since the dots of Langmuir model are regularly distributed besides de straight line. A different trend has been observed for Freundlich isotherm.

American Journal of Physical Sciences
ISSN: 2958-969X (Online)
Vol. 1, Issue 2, No. 1, pp 1 - 22, 2023
www.iprjb.org

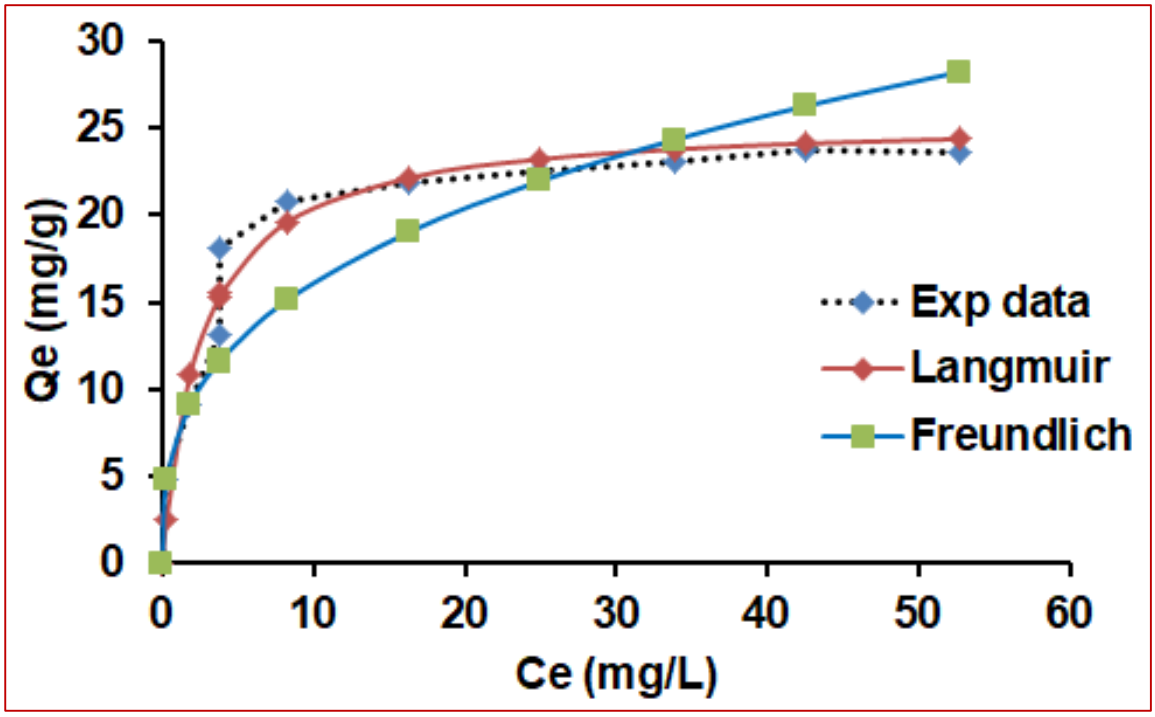

Figure 9: Plots of the Non-Linear Forms of Experimental Data, Langmuir and Freundlich Isotherms

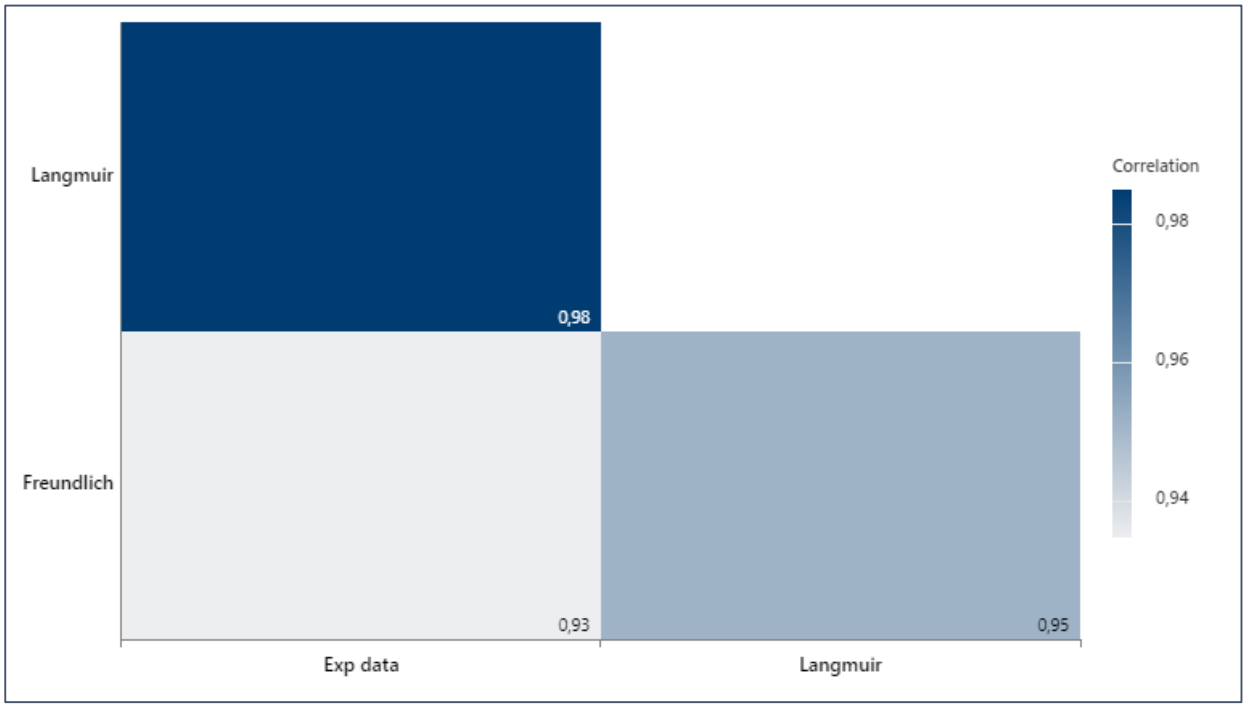

Figure 10: Correlogram Plots of Exp Data, Langmuir and Freundlich Models

Table 3: Equilibrium Constant of the Adsorption of NR4 onto SSC

Langmuir model		Freundlich model	
$\frac{C_e}{Q_e} = \frac{C_e}{Q_m} + \frac{1}{K_L Q_m}$		$logQ_e = \frac{1}{n} logC_e + logK_F$	
K_L (L/g)	0.402	K_F (mg/g/(L/mg)$^{1/n}$	7.457
Q_m (mg/g)	25.55	1/n	0.336
Q_e cal (mg/g)	23.64	R^2	0.93
R^2	0.98		
R_L	0.1 – 0.2		

Where Q_e is the amount of dye adsorbed per gram of adsorbent and C_e the concentration of the dye at equilibrium, Q_m the maximum amount of dye adsorbed, K_L and K_F are constant reflecting the affinity of the adsorbed species for the adsorbent.

American Journal of Physical Sciences
ISSN: 2958-969X (Online)
Vol. 1, Issue 2, No. 1, pp 1 - 22, 2023
www.iprjb.org

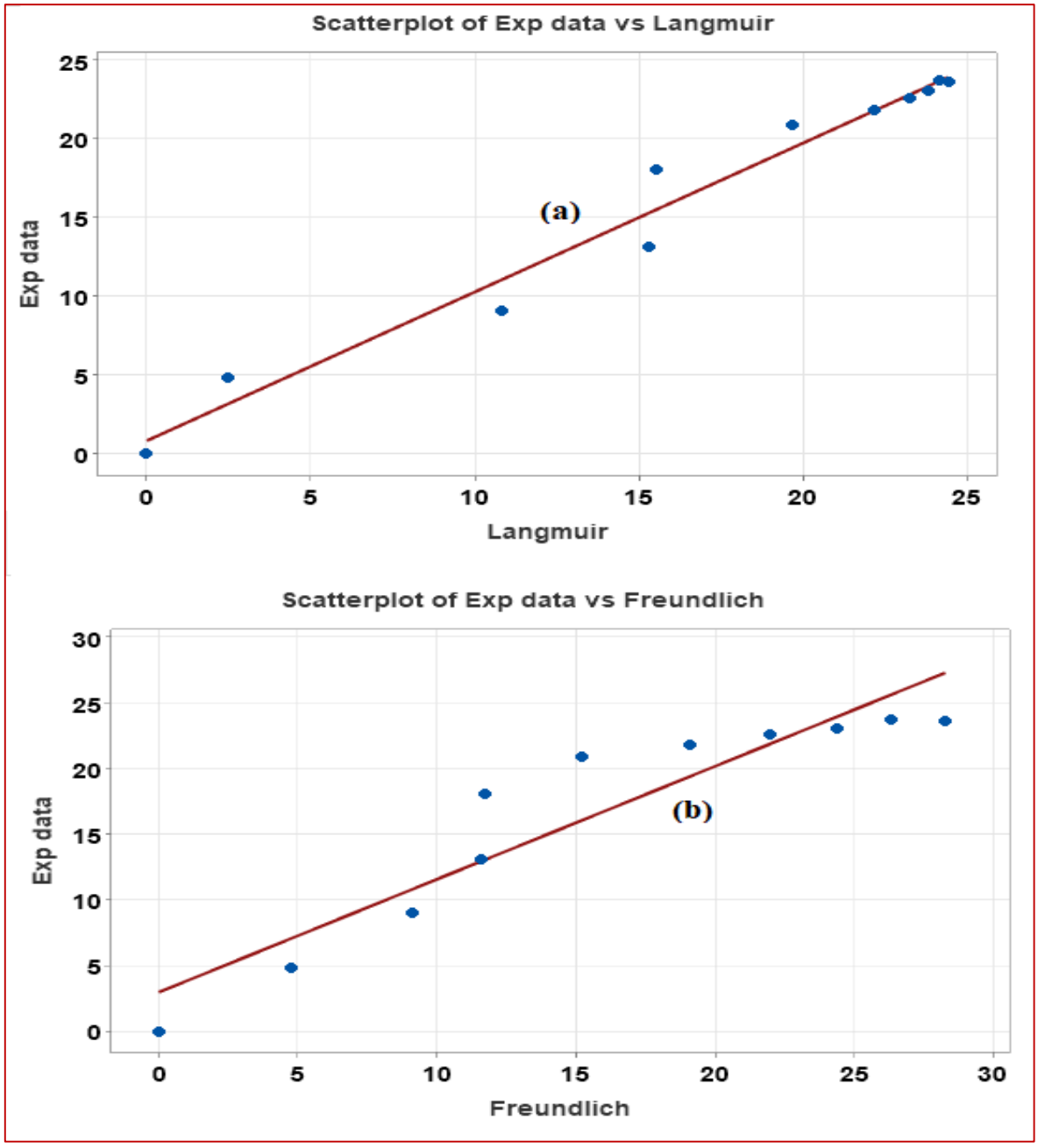

Figure 11: Scatterplots of Exp Data vs Langmuir Model (a) and Exp Data vs Freunglich Model (b)

Mechanism of Adsorption of NR4 onto SSC's Surface

Concerning the steps of the NR4 molecules adsorption onto SSC at the convenient pH range, the negatively charged NR4 molecules may firstly diffuse from the bulk solution towards the positively charged surface of SSC due to attractive coulombic forces. Secondly, the occurs fixation of dye molecules onto SSC positively charged surface through week interactions between the electrophile and negatives sites of the dye and silicon and aluminium cations atoms and other positives sites of the adsorbent. The suggested mechanism is illustrated on **Fig. 12.**

American Journal of Physical Sciences
ISSN: 2958-969X (Online)
Vol. 1, Issue 2, No. 1, pp 1 - 22, 2023
www.iprjb.org

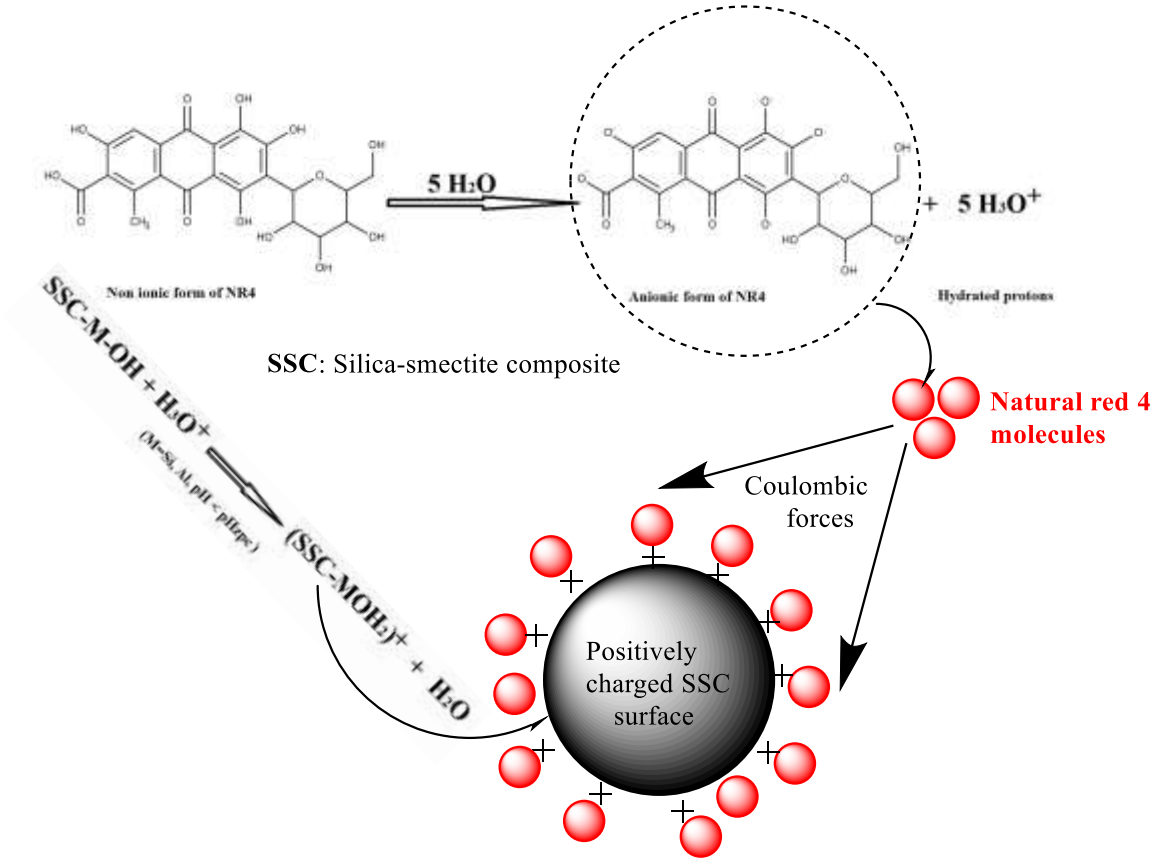

Figure 12: Illustration of Interactions between NR4 Molecules and SSC Surface

Recovery Results

Figure 9 shows that highest recovery is achieved with H_2O (38.7 %), followed by C_2H_5OH (35.20 %) and the lowest recovery is with H_2SO_4 (25.3%). The trend is strongly linked the pH of the medium. In fact, from the three solutions, the lowest pH corresponding to sulphuric acid contributes to increase the positive charge density and therefore favours to retain the NRA anionic molecules on the SCC surface. Reversely, when the pH increases from H_2SO_4 to C_2H_5OH, the recovery yield rises due to increasingly negative charges density on the SSC surface.

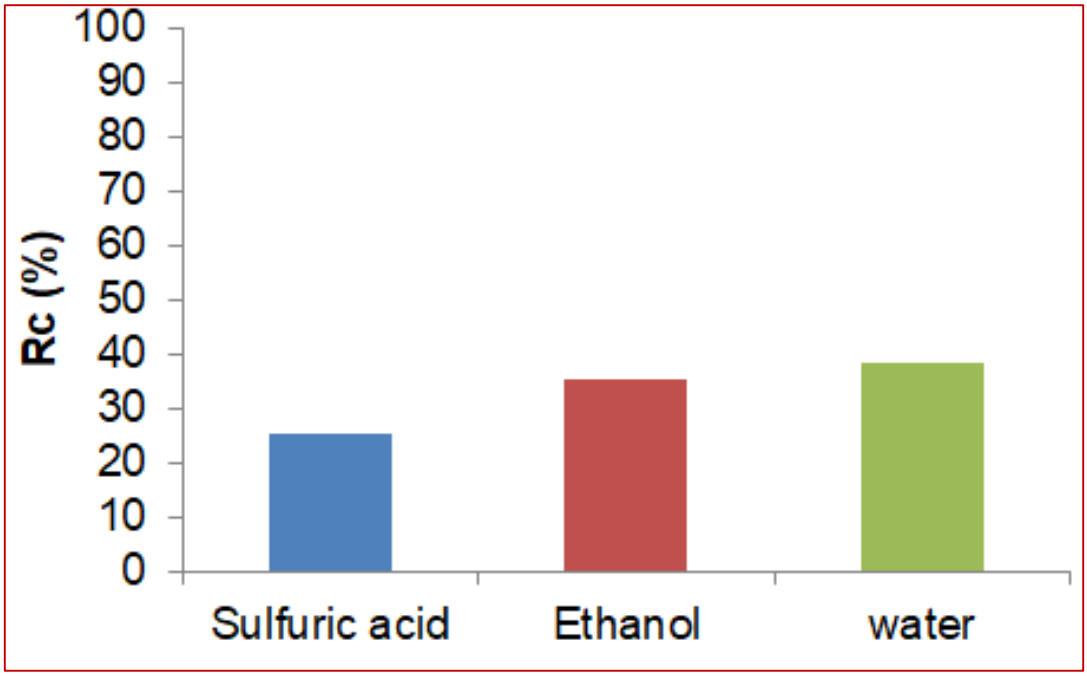

Figure 9: The effect of the Desorption Medium on NR4 from SSC.

Table 4 displays a comparative value of maximum adsorption capacity of NR4 onto various adsorbents found in the literature.

Table 4: Comparative Values of Sorption Capacities of NR4 onto Various Adsorbents

Adsorbent	Sorption capacity ((mg/g)	Source
Glass powder	4.04	[25]
Cu-Al-CLDH/CNT/PVDF400	33.44	[2]
Prunus mahaleb shell	148	[7]
Low-cost Silica-smectite composite	25.55	The present work
Activated carbon	4.16	[46]

The low-cost silica-smectite composite was more efficient than many other expensive adsorbents found in the literature

Conclusion

The removal efficiency of Natural red 4 dye by a low-cost silica-smectite clay (SSC) was studied experimentally and theoretically. Some processing parameters such as initial dye concentration, temperature, adsorbent dose, initial pH and contact time were varied from 10 -

50 mg/L, 25 – 65°C, 1 – 5 g/L, 4 - 8 and 0 - 120 min respectively. The thermodynamic parameters revealed that the NR4 adsorption onto SSC is endothermic and the process did not alter the structures of the adsorbent. The correlation of experimental data and kinetics models revealed that pseudo-first order and pseudo-second order had the best fitting with 0.99 and 0.98 as correlation values respectively. The accumulation of NR4 molecules at the surface of SSC followed Langmuir model isotherm with a maximum adsorption capacity Q_m of 25.55 mg/g. and a correlation value of 0.98 compared to 0.93 for Freundlich model.

Statements and Declarations

Conflicts of Interest

All authors certify that they have no affiliations with or involvement in any organization or entity with any financial interest or non-financial interest in the subject matter discussed in this manuscript.

Funding Statement

This research did not receive any specific grant from funding agencies in the public, commercial, or not-for-profit sectors

Authors Contributions

Jean Marie Kepdieu: Investigation, Roles/Writing - original draft, Data curation. **Chantale Njiomou Djangang**: Conceptualization, Methodology; Writing - review & editing, Visualization: Validation; Supervision. **Gustave Tchanang**, **Jacques Romain Njimou** and **Cyprien Joel Ekani**: Investigation,Writing - review & editing. **Sanda Andrada Maicaneanu** and **Chedly Tizaoui**: Methodology, Writing - review & editing.

REFERENCES

[1] F. J. Tuli, A. Hossain, A. K. M. F. Kibria, A. R. M. Tareq, S. M. M. A. Mamun, A. K. M. A. Ullah, *Environmental Nanotechnology, Monitoring & Management* **2020**, *14*, 100354.

[2] M. Abbasi, M. M. Sabzehmeidani, M. Ghaedi, R. Jannesar, A. Shokrollahi, *Journal of Molecular Liquids* **2021**, *329*, 115558.

[3] A. Atique Ullah, A. Fazle Kibria, M. Akter, M. Khan, A. Tareq, S. H. Firoz, *Water Conservation Science and Engineering* **2017**, *1*, 249.

[4] T. de Figueiredo Neves, N. B. Dalarme, P. M. M. da Silva, R. Landers, C. S. F. Picone, P. Prediger, *Journal of environmental chemical engineering* **2020**, *8*, 103820.

[5] E. Santoso, R. Ediati, Y. Kusumawati, H. Bahruji, D. O. Sulistiono, D. Prasetyoko, *Materials Today Chemistry* **2020**, *16*, 100233.

[6] S. A. Bhat, F. Zafar, A. H. Mondal, A. U. Mirza, Q. M. R. Haq, N. Nishat, *Journal of Cleaner Production* **2020**, *255*, 120062.

[7] Z. S. Keskin, Z. Mine Şenol, S. Kaya, S. Şimşek, *Journal of Molecular Structure* **2023**, *1275*, 134618.

[8] Y. Kuang, X. Zhang, S. Zhou, *Water* **2020**, *12*, 587.

[9] R. Javaid, U. Y. Qazi, A. Ikhlaq, M. Zahid, A. Alazmi, *Journal of Environmental Management* **2021**, *290*, 112605.

[10] S. Praveen, J. Jegan, T. Bhagavathi Pushpa, R. Gokulan, L. Bulgariu, *Biochar* **2022**, *4*, 10.

[11] E. Routoula, S. V. Patwardhan, *Environmental science & technology* **2020**, *54*, 647.

[12] S. De Jesús Méndez-Gallegos, R. Tiberi, T. Panzavolta, *Carmine Cochineal Dactylopius coccus Costa (Rhyncota: Dactylopiidae)* **2003**, 1000.

[13] T. Eisner, S. Nowicki, M. Goetz, J. Meinwald, *Science* **1980**, *208*, 1039.

[14] S. Kobylewski, M. F. Jacobson, *International journal of occupational and environmental health* **2012**, *18*, 220.

[15] A. Demirbas, *Journal of hazardous materials* **2009**, *167*, 1.

[16] W. Ruan, J. Hu, J. Qi, Y. Hou, C. Zhou, X. Wei, *Advanced Materials Letters* **2019**, *10*, 9.

[17] J. Abdi, M. Vossoughi, N. M. Mahmoodi, I. Alemzadeh, *Chemical Engineering Journal* **2017**, *326*, 1145.

[18] Z. Dehgani, M. Ghaedi, M. M. Sabzehmeidani, E. Adhami, *New Journal of Chemistry* **2020**, *44*, 13368.

[19] F. M. Mpatani, R. Han, A. A. Aryee, A. N. Kani, Z. Li, L. Qu, *Science of The Total Environment* **2021**, *780*, 146629.

[20] R. Bushra, S. Mohamad, Y. Alias, Y. Jin, M. Ahmad, *Microporous and Mesoporous Materials* **2021**, *319*, 111040.

[21] P. Verma, S. K. Samanta, S. Mishra, *Journal of Environmental Chemical Engineering* **2020**, *8*, 103851.

[22] J. M. Kepdieu, C. N. Djangang, J. R. Njimou, S. A. Maicaneanu, J. R. Mache, G. Tchanang, *Silicon* **2023**, 1.

[23] V. M. Vučurović, R. N. Razmovski, U. D. Miljić, V. S. Puškaš, *Journal of the Taiwan Institute of Chemical Engineers* **2014**, *45*, 1700.

[24] T. Gustave, D. Chantale Njiomou, A. Charles Fon, M. Danie Laure Mbella, D. Guillonnel Trésor Nyadjou, K. Jean Marie, et al., *Ann Civil Environ Eng* **2022**, *6*, 008.

[25] G. Atun, G. Hisarli, *Chemical Engineering Journal* **2003**, *95*, 241.

[26] M. P. da Silva, Z. S. B. de Souza, J. V. F. L. Cavalcanti, T. J. M. Fraga, M. A. da Motta Sobrinho, M. G. Ghislandi, *Environmental Science and Pollution Research* **2021**, *28*, 23684.

[27] A. Ahmad, C. Chan, S. Abd Shukor, M. Mashitah, *Chemical Engineering Journal* **2009**, *148*, 378.

[28] L. P. Vidoca, E. S. de Almeida, M. F. Cardoso, L. Otavio, L. F. Valadares, S. Monteiro, *Journal of Food Engineering* **2020**, *278*, 109944.

[29] M. A. Al-Ghouti, D. A. Da'ana, *Journal of Hazardous Materials* **2020**, *393*, 122383.

[30] J. M. Kepdieu, C. N. Djangang, G. Tchanang, J. R. Mache, C. F. Abi, P. Blanchart, *Journal of Chemistry* **2022**, *1*, 1.

[31] J. Nga, J. Avom, J. Tonga Limbe, D. Ndinteh, H. L. Assonfack, C. M. Kede, *Journal of Chemistry* **2022**, *2022*, 1.

[32] S. M. Silva, K. A. Sampaio, R. Ceriani, R. Verhé, C. Stevens, W. De Greyt, et al., *Journal of Food Engineering* **2013**, *118*, 341.

[33] B. M. J. Baptiste, B. K. Daniele, E. M. Charlène, T. T. L. Canuala, E. Antoine, K. Richard, *Scientific African* **2020**, *9*, e00498.

[34] G. Lente, I. Fábián, A. J. Poë, *New Journal of Chemistry* **2005**, *29*, 759.

[35] I. Santamaría-Holek, A. Pérez-Madrid, *The Journal of Chemical Physics* **2020**, *153*.

[36] M. C. Ncibi, B. Mahjoub, M. Seffen, *rseau* **2008**, *21*, 441.

[37] B. H. Hameed, R. R. Krishni, S. A. Sata, *Journal of Hazardous Materials* **2009**, *162*, 305.

[38] S. Al-Mahmoud, *Egypt. J. Chem.* **2020**, *0*, 0.

[39] Sumanjit, S. Rani, R. K. Mahajan, *Arabian Journal of Chemistry* **2016**, *9*, S1464.

[40] J. Baliti, A. Asnaoui, S. Abouarnadasse, International Journal of Innovative Research in Advanced Engineering **2014**, 1, 313.

[41] K. M. Kifuani, A. Kifuani Kia Mayeko, P. Noki Vesituluta, B. Ilinga Lopaka, G. Ekoko Bakambo, B. Mbala Mavinga, et al., Int. J. Bio. Chem. Sci **2018**, 12, 558.

[42] D. Sarkar, D. Chattoraj, Journal of colloid and interface science **1993**, 157, 219.

[43] S. K. Parida, B. K. Mishra, *Journal of colloid and interface science* **1996**, *182*, 473.

[44] A. Abdullahi, U. Abubakar, M. K. Sani, M. Yusuf, *Studies* **2022**, *1*.

[45] M. Gonbadi, S. Sabbaghi, R. Saboori, A. Derakhshandeh, M. Narimani, A. Fatemi, *International Journal of Environmental Science and Technology* **2023**, *20*, 3101.

[46] A. Thakur, S. Kaya, A. S. Abousalem, A. Kumar, *Sustainable Chemistry and Pharmacy* **2022**, *29*, 100785.